# Using Gene Expression Programming to Determine the Impact of Minerals on Erosion Resistance of Selected Cohesive Egyptian Soils

**Ahmed M. A. Sattar**

**Abstract** Cohesive sediment soils are encountered throughout Egypt at many locations, posing various physical and chemical characteristics in beds of lakes, estuaries and flash flood flows. The entire delta region is made up of clayey soil formed from various consecutive Nile floods before construction of the High Dam. Thus, it is very important to determine the erosional stability of such cohesive soils as a function of sediment chemical properties and mineral content. In the current research, 48 samples are collected from various locations throughout Egypt. All samples are subject to physical tests for grain size distribution, and X-ray diffraction analysis for mineral contents. Laboratory experiments are carried out on these samples for finding the difference in terms of erosion characteristics caused by different sediment composition among all samples. Assuming other properties of cohesive soils constant, the gene expression programming (GEP) algorithms are applied to relate the clay mineral content to experimental critical shear stress. Results show an excellent potentiality for the GEP for being applied on finding relations between complex parameters with nonlinear relationships with respect to soil erosion.

## 1 Introduction

One of the most important factors controlling the interaction of flow and the evolution/change of bed morphology as a result of such flow is the soil erodibility, i.e., the potential for soil surface to being transported by the moving water. This

A. M. A. Sattar (✉)
Department of Irrigation & Hydraulics, Faculty of Engineering,
Cairo University, Orman Street, Giza, Egypt
e-mail: ahmoudy77@yahoo.com

erodibility is linked to the water velocity and, therefore to the shear stresses that erode soil. The soil erodibility is directly related to the soil grain size (especially for non-cohesive soil), i.e., larger soil particles need higher velocity for removal and transport. Non-cohesive soils represent sandy type soils, and Hydraulic Engineering Circular, HEC-18 (FHWA 2001) contains several established erodibility models for non-cohesive soils. Richardson and Davis (1995) presented various established scour predictors for sandy soils. However, sandy soils are only available on the shores of Egypt, while the entire delta region is made up of clayey soil formed from various consecutive Nile floods before construction of the High Dam (a pivot of Egypt industrialization, controlling flood waters and generating hydropower, www.en.wikipedia.org/wiki/Aswan_Dam) posing various physical and chemical characteristics in beds of lakes, estuaries and flash flood flow areas. The clayey soil found mostly in the delta region is considered to be from the cohesive type soil. Cohesive type soils follow an opposite regime with respect to erodibility than non-cohesive soils, where cohesive soils erosion resistance increase with the decrease in particle diameter and thus increase in plasticity. Many attempts have been made to correlate critical shear stress with various common parameters of cohesive soils (water content, unit weight, plasticity index, percent of silt and clay particles by weight passing sieve # 200, undrained shear strength) leading to the development of a database of 91 Erosion Function Apparatus (www.humboldtmfg.com/pdf2/hm4000ds.pdf) EFA tests, which was used to perform regression analyses and obtain correlation equations; however, all attempts failed to reach a model that describes the various contributing parameters with reasonable value for the coefficient of determination, *R-squared* (Cao et al. 2002). Other phenomena impact the erosion properties of cohesive soils, such as those developing when clay dries, and diagenetic bonds due to aging, such as those developing when clay turns into rock under pressure over geologic time. Due to the complexity of interaction between these parameters, it is very difficult to predict critical shear stress empirically on the basis of few properties. However, investigating the impact of such parameters individually on the erosion resistance of cohesive soils remained a topic that is frequently visited. Many researchers studied the impact of individual parameters on the erosion resistance of cohesive soils (mainly clay) and reported some empirical formulas, e.g., Dunn (1959); Enger et al. (1968), Hydrotechnical, Lyle and Smerdon (1965); Smerdon and Beasly (1959); Arulanandan (1975); Kelly and Gularte (1981) and Cao et al. (2002). Many of the related parameters were studied thoroughly except for the mineral content of clay, which did not receive such attention and thus in various reports the impact of many soil parameters on critical shear stress is documented, with no data on the impact of soil minerals as seen in Table 1 (Independent Levee Investigation Team 2006).

Recently, evolutionary algorithms have been used as a superior alternative for regression analysis and artificial neural networks, for finding relations between various parameters and producing a higher R-squared value and less mean error in prediction using a newly developed equation. Applications of evolutionary algorithms, especially gene expression programming (GEP) in water and environmental engineering, are not as numerous as the other soft computing tools of

**Table 1** Impact of various soil parameters on critical shear stress of cohesive soils (clay)

| When parameter increases | Erosion change |
| --- | --- |
| Unit weight | Decreases |
| Plasticity index | Decreases |
| Undrained shear strength | Increases |
| Void ratio | Increases |
| Swell | Increases |
| Percent passing sieve #200 | Decreases |
| Clay minerals | —— |

artificial neural networks. They are restricted to finding functions in relatively fewer sub-areas including scour prediction downstream of hydraulic structures (Guven and Gunai 2008), stage discharge relationship prediction (Guven et al. 2009), predicting sediment transport in sewer pipe systems (Ghani and Azamathulla 2011), and prediction of bridge pier scour (Azmathulla et al. 2009).

This chapter aims at experimentally investigating the impact of various mineral constituents on the critical shear stress for soil erosion for selected Egyptian cohesive soils using experimental methods and novel evolutionary algorithms known as GEP, to relate various mineral constituents to the critical shear stress. First, an overview of the basic theory of gene expression programming is given, accompanied by implementation technique steps. Afterwards, a description for the experimental setup used to collect erosion data is given with the results. Key parameters considered are the mineral constituents of the soil samples with most of the other parameters either constant or have little variation.

## 2 Gene Expression Programming

Gene expression programming was invented by Ferreira in 1999, and is the natural development of genetic algorithms, GAs and genetic programming GP. GEP uses the same kind of diagram representation of GP, but the entities produced by GEP (expression trees) are the expression of a genome. Therefore, with GEP, the second evolutionary threshold—the Phenotype Threshold—was crossed, providing new and efficient solutions to evolutionary computation. So, the great insight of GEP consisted in the invention of chromosomes capable of representing any expression tree. GEP is a full-fledged genotype/phenotype systems, with the genotype completely separated from the phenotype, thus it surpasses the GP system by a factor of 100–60,000 (Ferreira 2001).

The fundamental difference between GP and GEP resides in the nature of the individuals forming the expression trees (Fig. 1). In GP, the individuals are nonlinear entities of different sizes and shapes called parse trees (or expression tree) that represent a program/function, while in GEP, the individuals are also nonlinear entities of different sizes and shapes, Expression Trees ET, but these complex entities are encoded as simple strings of fixed length (chromosomes).

**Fig. 1** Expression tree representation for a function



Function: $(a + b) * \sqrt{b - c}$
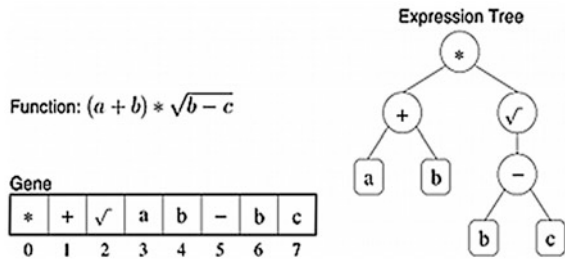
Initially, the chromosomes of each individual in the population are generated randomly. Furthermore, the structure of chromosomes was designed to allow the creation of multiple genes, each encoding a sub-expression tree. The genes are structurally organized in a head and a tail, and it is this structural and functional organization of GEP genes that always guarantees the production of valid programs, no matter how much or how profoundly the chromosomes are modified. The individuals in the new generations are subject to development processes such as expression of the genomes, confrontation of the selection environment, and reproduction with modifications. These processes are repeated for a predefined number of generations or until a solution is achieved as shown in the GEP flow chart in Fig. 2 (Ferreira 2001).

GEP evolves computer programs to solve problems by executing the following steps (Ferreira 2001);

*Step*1: One (or more) initial population of individuals is randomly generated with functions and terminals related to the problem domain.

*Step*2: The implementation of GEP iteratively performs the following steps until the termination criterion has been satisfied

(1) The fitness function for every individual is estimated to enable program to find solution by itself.
(2) Chromosomes are created by choosing a set of terminals and appropriate functions.
(3) The chromosome architecture is chosen including the length of the head and the number of genes.
(4) The linking function is set for Expression Trees, ETs.
(5) The next generation is produced using the genetic operations (reproduction, crossover and mutation).
(6) The termination criterion is checked. If it is not satisfied, the next iteration is performed; if satisfied, go to step 3.

*Step*3: The result may be a solution to the problem domain.

The GEP fitting for the experimental data is done using the commercial software GenXProTools, unconstrained and non-linear data mining software (www.gepsoft.com).
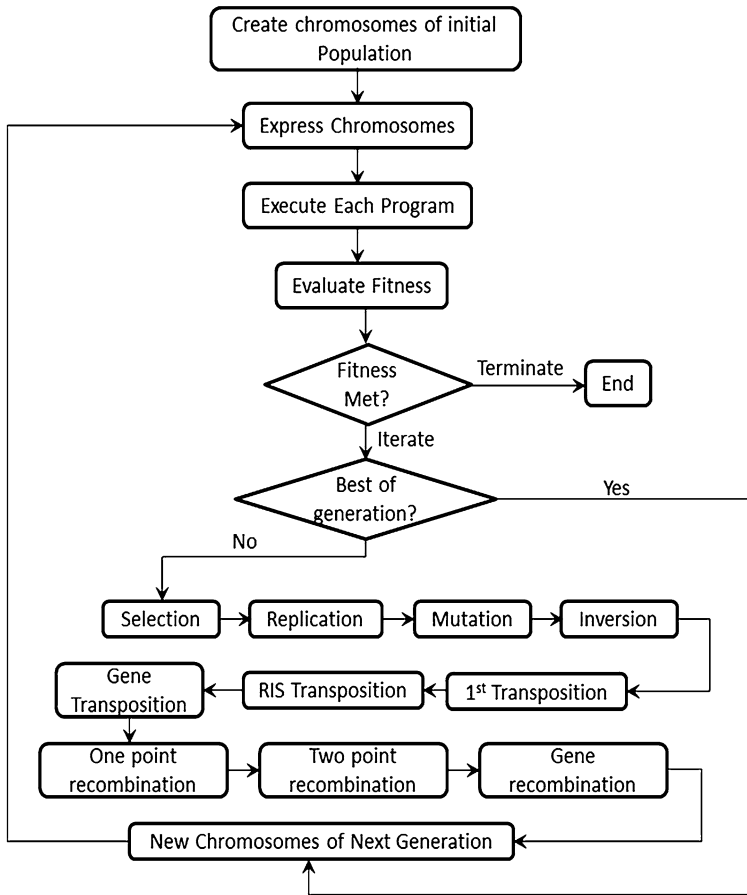
**Fig. 2** Flow chart of gene expression programming (Ferreira 2001)

# 3 Experimental Setup

The experiments are performed in a straight flume (Fig. 3), which is located at the Irrigation and Hydraulics Department at Cairo University. The flume is composed of steel skeleton with steel sheeting for the bed and plexiglass on both sides; it is fed through a small centrifugal pump with a capacity of 150 L/s, through 8 inch UPVC pipes. Water is circulated through the flume and then to the below tanks beside the flume and mounted on the surface of the lab. The flume is 12 m long, 1.2 m deep and 0.30 m wide with adjustable bed slope that is set to 1/200 and an average water depth of 0.40 m. The average manning roughness coefficient of bottom and wall was calculated from velocity to water surface profile measurements and is found to be approximately 0.01. The discharge is measured by an orifice plate and a manometer installed on pipe on pump discharge side. Flow
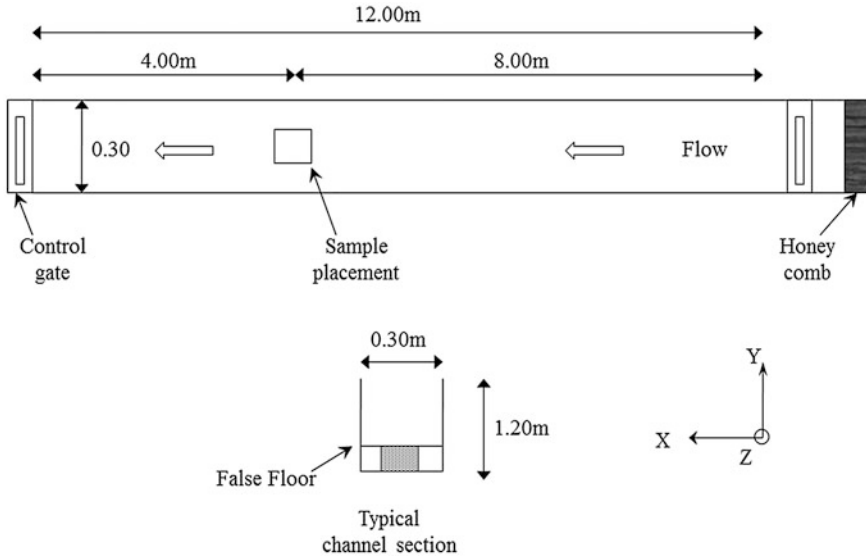
**Fig. 3** Experimental setup for bed erosion experiments

velocity and depth are controlled in the flume by gate valve on the pump discharge side and a downstream sluice gate. The downstream end of the flume is left opened with an adjustable tailgate for controlling the water level in the channel downstream. To ensure properly developed flow at the breach location, perforated screens and 60 mm long honeycomb are places at the flume inlet. A point gauge is used to measure water surface in channel with an accuracy of 0.1 mm on vernier scale. A 10 MHz 3D nortek acoustic doppler velocimeter (ADV) is used to measure 3D velocity and turbulent components of flow fields.

For the purpose of conducting erosion tests for cohesive soils, procedures and test preparation are considered as in Salaheldin et al. (2004), who presented methodology for prediction of erosion resistance and pattern for cohesive soils. Their methodology operates on both undisturbed and remolded samples; they suggested sample size and procedure for sample placement and onset of erosion of sediment sample. Their procedure extends the erosion resistance determination by scaling it up to prototype scale, yielding very similar results thereby indicating that the methodology is not scale dependent. A false bottom is constructed over the bed of the existing flume with a height of 8 cm above flume bottom and with width less than the flume width by 1 cm to allow for placement in lab flume. The false bottom is intended to enable placing a 20 × 20 cm steel box flushed with the false floor for placement of cohesive soil samples in. The sample box has sides completely flushed with the false floor and placed at 8 m from the inlet of the flume to have fully developed flow. The soil was initially trimmed flush with the bottom of the flume at the location of the sample. Flow is gradually increased for steps and each flow is maintained for a sufficient period of time to cause erosion and, if

erosion does not occur, the flow is further increased for the same amount of time until the erosion is observed and water becomes muddy; this time is taken to be 2 h (Salaheldin et al. 2004). The initiation of erosion is determined visually and in conjunction with the formation of a small cloud of mud in water, the erosion always starts from the upstream side of the sample.

Unlike the velocity measurements that needed only 2,000 sample to be accurately determined, the turbulence parameters of flow need at least 5,000–10,000 sample. Critical bed shear stress at the onset of erosion of cohesive sediment sample is determined in this study using the covariance method (COV). The COV is considered to give unbiased estimates of $\tau$ among the different methods available to estimate $\tau$ from velocity measurements. Instantaneous velocities measured by the ADV are used to obtain the instantaneous random fluctuation terms such that $u' = U - \bar{U}$, $v' = V - \bar{V}$, $w' = W - \bar{W}$. The local mean covariance, $\overline{u'w'}$, $\overline{u'v'}$, $\overline{v'w'}$, is called Reynolds stress and used for fully turbulent flow to calculate the near bed shear stress through $\tau = -\rho\left(\overline{u'w'}\right)$.

Undisturbed field soil samples that are used are collected from several locations covering all various types of cohesive soils in Egypt from north to south. Samples were collected from Aswan, Kafr ElSheikh, Shark El Tafreea, and Fayoum. These samples are manually collected in big chunks, the surface layer is removed since it is disturbed and contains debris, and then each chunk is cut into pieces of $40 \times 40$ cm and soil is shoveled to a depth of 20 cm and scooped from the bottom. Samples are protected with plastic and in lab are cut with sharp knives to fit in the flume groove. From each location, various samples are collected and tested. Tests include grain size distribution, compaction tests, water content; and to determine the mineral composition of soil samples, X-Ray Diffraction analysis was performed.

## 4 Results and Discussions

To ensure repeatability of experiments and determine error in velocity measurements, the experiment was run for several times and velocity components at a selected location have been recorded; it was found that experiments are repeatable and error in velocity measurements was less than 1 %. On the other hand, bed shear stress as calculated by the COV method has been recorded for various soil samples and ranged between 0.9 and 2.6 Pascal. Table 2 shows the critical shear stress range obtained from this experiment versus that obtained by others for cohesive soils. X-Ray Diffraction (XRD) analysis was performed on all samples to determine the mineral composition of selected cohesive soils in Egypt. The cohesive soils had colors from grey to reddish brown according to the location and had considerable variations in mineral contents, as shown in Fig. 4.

Thus, for each sample, we have the mineral composition—in percentages of various minerals as obtained from the XRD—and the corresponding critical shear

**Table 2** Critical shear stress as obtained by various researchers for clay

| Study | $\tau_{critical}$(Pa) |
|-------|----------------------|
| Dunn (1959) | 2–25 |
| Enger et al. (1968) | 15–100 |
| Lyle and Smerdon (1965) | 0.35–2.25 |
| Smerdon and Beasley (1959) | 0.75–5 |
| Arulanandan et al. (1975) | 0.1–4 |
| Arulanandan (1975) | 0.2–2.7 |
| Kelly and Gularte (1981) | 0.02–0.4 |
| Current study | 0.9–2.6 |
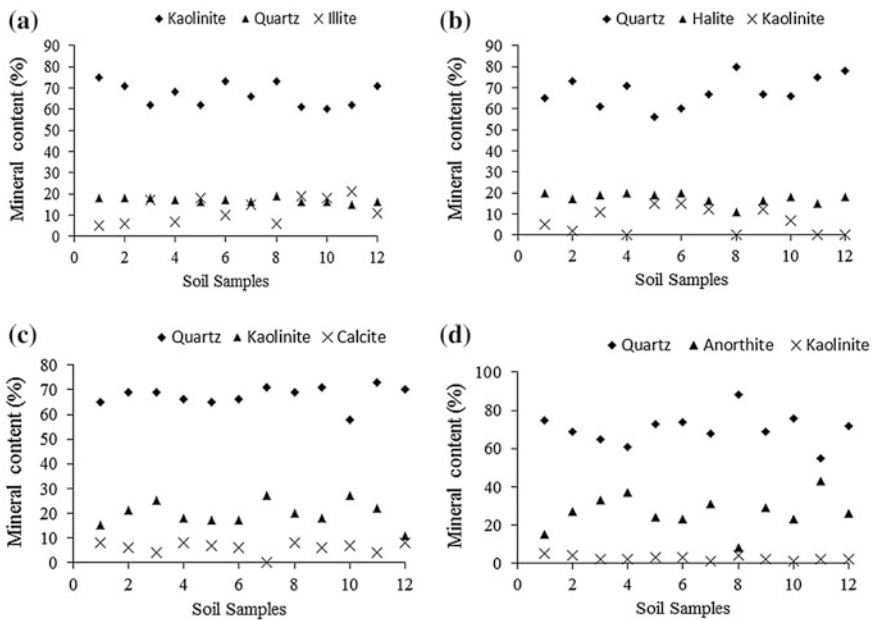


**Fig. 4** Mineral composition of selected soil samples at **a** Aswan, **b** Shark El tafreea, **c** Fayoum, **d** Kafr ElSheikh

stress at the onset of initiation of erosion. As mentioned before, this study is concerned about the mineral content of the clay and thus minerals are the only parameters assumed to affect the initiation of erosion. Other parameters, such as grain size, water content, and density were measured and variation is not observed to be significant amongst all samples. The critical shear stress for clay samples can be written as follow;

$$\tau_{critical} = f\{Kaolinite, Quartz, Halite, Illite, Calcite, Chlorite, Montmorillonnite\}$$

$$(1)$$

To apply the GEP, we need to define the learning environment using a fitness function, as suggested by Ferreira (2001). Previous experience with the GEP

suggests the choice of root relative squared error (RRSE) as a fitness function; it helps an efficient evolution for the model and allows it to travel fitness landscape until it finds an optimal solution for the given problem. This function computes the total squared error and normalizes it by the same dimensions as the quantity being predicted; the root relative square error $E_i$ of an individual program $i$ is defined by the following equation;

$$E_i = \sqrt{\frac{\sum_{j=1}^{n}\left(P_{(ij)} - T_j\right)^2}{\sum_{j=1}^{n}\left(T_j - \bar{T}\right)^2}} \tag{2}$$

Where $P_{(ij)}$ is the value predicted by the program $i$ for fitness case $j$; $T_j$ is the target value for fitness case $j$; and $\bar{T} = 1/n \sum_{j=1}^{n} T_j$. For a perfect fit $E_i = 0$, and thus the index of RRSE ranges from 0 to infinity, with zero corresponding to the ideal. Thus, the fitness of an individual model $f_i$ can be calculated from the following equation which ranges from 0 to 1,000, with 1,000 corresponding to perfect fit;

$$f_i = 1000.\frac{1}{1 + E_i} \tag{3}$$

The second step is to choose the chromosome architecture; this includes determining the number of chromosomes, head size and number of genes. Each gene is composed of a head and a tail; the head contains symbols that represent a chosen function and the tail contains terminals. The length of the head $h$ is chosen such that it controls the size of the formed expression trees; the tail $t$ is a function of the head size and of the number of functions chosen $n$, such as $t = h (n - 1) + 1$. Several trials with various head sizes need to be attempted to reach for the best fitness and an optimum head. From practice with various problems, a head size of three to five will always give the best models with respect to size and predictability.

The GEP chromosomes are composed of one or more genes of equal length. Each gene codes for a sub-expression tree and each of the sub expression trees interact with each other, forming more complex expression trees. Choosing one gene leads to a complex expression tree, while multigenic chromosomes are always preferred in complex problems with nonlinear relations, where each gene codes for a smaller and simpler building block. The gene number is determined by trial runs and in general two to six genes will be more than sufficient in problems with various complexities.

The third step is choosing the set of functions that will create the chromosomes. These functions are the essence of evolution of the GEP; they allow modifications without restrictions leading to compact correct programs for a specific function. The choice of an appropriate function set is not the same for every problem and depends mainly on the program performance with some chosen arguments. If the evolution is not satisfactory, one can use a wider set of functions until optimum fitness is achieved. However, a professional approach would be to initially use the

**Table 3** Optimal parameter settings for the GEP algorithms

| Parameters | Settings-GEPI | Settings-GEPII |
|---|---|---|
| Number of generations | 100,000 | 100,000 |
| Number of chromosomes | 30 | 30 |
| Number of genes | 3, 4 | 3, 4 |
| Head size | 3, 5, 8 | 3, 5, 8 |
| Linking function | Addition | Addition |
| Fitness function error type | RRSE | RRSE |
| Mutation rate | 0.05, 0.005 | 0.05, 0.005 |
| Inversion rate | 0.1 | 0.1 |
| One point recombination rate | 0.3 | 0.3 |
| Two Point recombination rate | 0.3 | 0.3 |
| Gene recombination rate | 0.1 | 0.1 |
| Gene transposition rate | 0.1 | 0.1 |
| Function set | $+, -, \times, /, \sqrt{}, $ e, In | $+, -, \times, /, \sqrt{}, $ e, In, cos, sin, arctan, $1/$ |

basic mathematical operators $(+, -, \times, /)$ to allow for production of simple models. A second run of GEP is performed using a different set of functions as shown in Table 3.

The fourth step is to set the linking function, which is the interaction between all sub-expression trees of the model, these linking functions can be addition, subtraction, division, and multiplication. Obviously, it works only in case of multigenic models. The choice of linking functions depends on the complexity of the problem and the experience of the model user and for simpler models for a certain problem, addition or subtraction would be appropriate.

The fifth step is to set the values controlling various genetic operations controlling the evolutionary process of GEP. The most efficient operator in GEP is the mutation, which causes populations of individuals to adapt very efficiently, allowing for the evolution of good solutions to all problems. Ferraire (2001) recommends using a mutation rate equivalent to two one-point mutations per chromosome. Mutations cause the expression trees to drastically change in size with no constraints in kind of mutation and number of mutations in a chromosome. Other genetic operations, such as inversion, transposition, and other operators shown in the above flow chart, are of less importance and all depend on the value assigned for mutation rate. Thus, default values are always assigned for all genetic operations, as shown in Table 3, and the value of the mutation rate changes from 0.05 to 0.005 to test the evolution of the program.

To test the performance of the developed model, the mean square error, MSE, mean absolute error, MAE, and relative squared error, RSE, were used as indicators, as calculated from the following equations, respectively

$$MSE_i = \frac{1}{n} \sum_{j=1}^{n} \left( P_{(ij)} - T_j \right)^2 \qquad (4)$$

**Table 4** Performance of produced functions for critical shear stress

| Performance indicators | GEPI | GEPII |
|---|---|---|
| Fitness | 780 | 756 |
| MSE | 0.0139 | 0.0158 |
| MAE | 0.0946 | 0.0946 |
| RSE | 0.09131 | 0.1036 |
| R-Square | 0.942 | 0.89 |

$$MAE_i = \frac{1}{n}\sum_{j=1}^{n}\left|\frac{P_{(ij)} - T_j}{T_j}\right| \tag{5}$$

$$RSE_i = \frac{\sum_{j=1}^{n}\left(P_{(ij)} - T_j\right)^2}{\sum_{j=1}^{n}\left(T_j - \bar{T}\right)^2} \tag{6}$$

Results from both models; GEPI and GEPII, are shown in Table 4. According to Table 4, GEPI model with chosen set of functions produced the best results with a fitness value of 780 and an R-Square value of 0.94. On the other hand, GEPII model with sin, cos and arctan, did not produce results with same accuracy. Both models evolved with four genes and thus each function produced has four expression trees. All expression sub trees are linked by addition and the gene mutation was run using random constants for each gene. The best individual of all generations for GEPI has the explicit formulation as follows

$$\tau_{critical} = e^{\left\{Cl^3/(Kt \times Q - Cl)\right\}^9} - 0.85819\sqrt{Il} + 2M + 0.795014 + Kt^2 \times Q^2 - Kt$$
$$- 137.684Q \times M(Il - Ca) - Ca$$
$$+ H^3\left[(Kt - Q)^2 + 64.444 + 16.0557(Kt - Q)\right] \tag{7}$$

where all minerals are in percentages and $\tau_{critical}$ is in Pascal; $Q$ = quartz, $Kt$ = kaolinite, $Cl$ = chlorite, $Il$ = ilite, $M$ = montmorillonite, $H$ = halite, and $Ca$ = calcite.

On the other hand, simpler equations can be obtained using the GEP when only one gene is specified as the main chromosome architecture with rest of parameters as in GEPI; however, the fitness of the model decreased to 745 with MAE of 0.105 and R-squared of 0.89; the following figure shows the architecture of the single genetic expression tree;

According to the ET in Fig. 5, the equation is further simplified to

$$\tau_{critical} = M + Q - Kt + 0.44451Ca - 0.884949 - Ca \times Q$$
$$+ [M - Il + 5.947266Q]^3 \tag{8}$$

where $Q$ = quartz, $Kt$ = kaolinite, $Cl$ = chlorite, $Il$ = ilite, $M$ = montmorillonite, $H$ = halite, and $Ca$ = calcite.
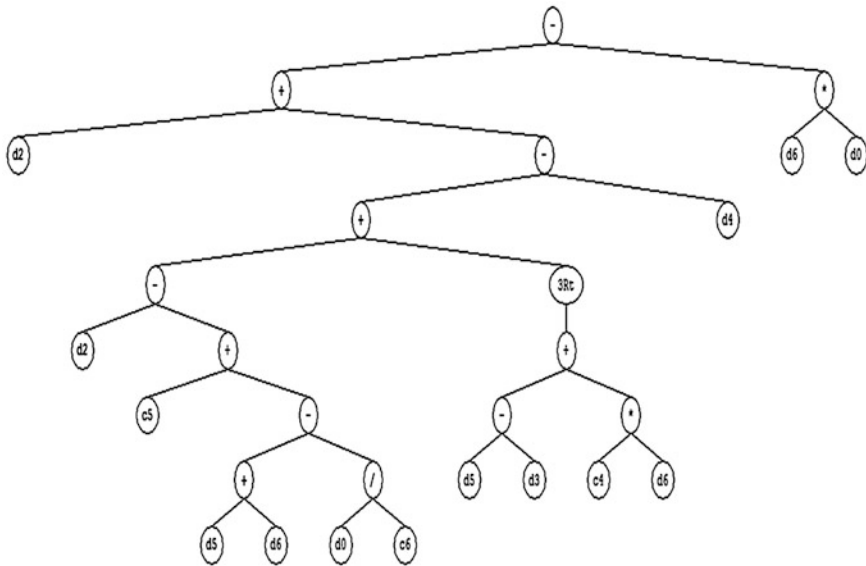
**Fig. 5** Expression tree produced by the GEPI, 1 gene used

As interpreted from the simplified equation, the critical shear stress for clay depends on all minerals in the clay samples and thus its increase cannot be attributed alone to the increase or decrease in a certain mineral. It is found that the clay samples of Shark El Tafreea had the highest critical shear stress amongst all other samples with an average value of 2 Pa. The main constituent of this sample is quartz, followed by halite and kaolinite. On the other hand, the lowest shear stress with an average value of 0.9 Pa was in the samples collected from Aswan having kaolinite as major constituent followed by quartz and illite. Other soil parameters are assumed to be constant such as water content and density.

## 5 Conclusions

The results show that gene expression programming (GEP) is capable of mapping data into a high dimensional feature space with variety of methods to find relations and trends in data. An equation linking the critical shear stress in clays with the mineral composition has been presented and MAE reached less than 0.09. Despite the fact that none of the other parameters, such as water content, percent passing sieve 200, density, swelling, etc., has been included, the relation can be used to provide estimates for critical shear stress versus soil type in Egypt, according to soil mineral composition and location of samples.

# References

Arulanandan K (1975) Fundamental aspects of erosion in cohesive soils. J Hydr Div 101(5):635–639 (ASCE)

Azamathulla H, Ghani AA, Zakaria N, Guven A (2009) Genetic programming to predict bridge pier scour. J Hydraul Eng 136(3) (ASCE)

Cao Y, Wang J, Briaud JL, Chen HC, Li Y, Nurtjahyo P (2002) EFA tests and the influence of various factors on the erodibility of cohesive soils. In: Proceedings of the first international conference on scour of foundations, Texas A and M University, Department of Civil Engineering, College Station

Dunn IS (1959) Tractive resistance to cohesive channels. J Soil Mech Found Div 85(3):1–24 (ASCE)

Enger PF, Smerdon ET, Masch FD (1968) Erosion of cohesive soils. J Hydr Div 94(4):1017–1049 (ASCE)

Federal Highway Association FHWA (2001) Evaluation scour at bridges. Tech Circular 4th edn Pub. # NHI 01-001, US Department of Transportation

Ferreira C (2001) Gene expression programming: a new adaptive algorithm for solving problems. Complex Syst 13(2):87–129

Ghani AA, Azamathulla H (2011) Gene expression programming for sediment transport in sewer pipe systems. J Pipeline Syst Eng Pract 2(3):102–106

Guven A, Gunai M (2008) Genetic programming approach for prediction of local scour downstream of hydraulic structures. J Irrig Drainage Eng 134(2):241–249

Guven A, Aytek A, Yuce MI, Aksoy H (2009) Genetic programming based empirical model for daily reference evapotranspiration estimation. Clean: Soil Air Water 36(10–11):905–912

Independent Levee Investigation Team (2006) Investigation of the performance of the new orleans flood protection systems in hurricane katrina on August 29, 2005. Vol I. Main Tests and Executive Summary

Kelly EK, Gularte RC (1981) Erosion resistance of cohesive soils. J Hydr Div 107(10): 1211–1224 (ASCE)

Lyle WM, Smerdon ET (1965) Relation of compaction and other soil properties to erosion and resistance of soils. Trans Am Soc Agric Eng 8(3). St Joseph Michigan

Richardson EV, Davis SR (1995) Evaluating scour at bridges. Rep. No. FHWAIP—90-017 (HEC 18), Federal Highway Administration, Washington

Salheldein T, Imran J, Chaudhry H (2004) Numerical modeling of three dimensional flow field around circular piers. J Hydraul Eng 130(2) (ASCE)

Smerdon ET, Beasley RP (1959) Tractive force theory applied to stability of open channels in cohesive soils. Res Bull No 715, Agricultural Experiment Station, University of Missouri, Columbia